

**B. Imansakipova**<sup>1</sup>,  
orcid.org/0000-0003-0658-2112,  
**I. Vassilyev**<sup>2</sup>,  
orcid.org/0000-0002-6216-0443,  
**Sh. Aitkazanova**<sup>\*1</sup>,  
orcid.org/0000-0002-0964-3008,  
**M. Kalipanov**<sup>3</sup>,  
orcid.org/0000-0003-2974-1083,  
**K. Issabayev**<sup>3</sup>,  
orcid.org/0000-0001-5183-3668

1 – Satbayev University, Almaty, Republic of Kazakhstan  
2 – Special Design and Technology Bureau “Granit”, Almaty, Republic of Kazakhstan  
3 – Institute of Machine Science and Automation of the National Academy of Sciences of Kyrgyz Republic, Bishkek, Kyrgyz Republic  
\* Corresponding author e-mail: [sh.aitkazanova@satbayev.university](mailto:sh.aitkazanova@satbayev.university)

## IDENTIFICATION AND SUPPRESSION OF SIGNALS OF THE REAR LOBE OF THE RADIATION PATTERN OF THE RADAR ANTENNA

**Purpose.** Development of a new approach to improving the accuracy of orientation based on radar reflections from local objects and a digital terrain model.

**Methodology.** The research is based on the theory of radiation, reflection and reception of radar signals. Statistical analysis of a large volume of recorded signals establishes causal relationships between the appearance of “false” reflections formed by the back lobe of the radiation pattern and to develop a computational algorithm for their suppression.

**Findings.** A method and software that allows detecting and suppressing “false” reflections formed by the rear lobe of the antenna pattern without distorting the reflections created by the main lobe. For this purpose, a criterion has been developed, determined by the ratio of the amplitude of the signal received by the front lobe to the amplitude of the signal recorded by the rear lobe. The criterion allows eliminating the “false” signals without having a priori information about the real radiation pattern using a regulator for the reduction of phantom reflections to an average noise level.

**Originality.** For the first time, suppression has been carried out of “false” reflections without having a priori information about the real radiation pattern of the radar station antenna, as well as elimination of the loss of informativeness of the real reflection formed by the main lobe.

**Practical value.** A method is suggested of radar immunity of radar stations is noise immunity due to “false” reflections. The potential of the method and the capabilities of the developed computer program determines the relevance of their capabilities for use by all radar stations at various frequencies, azimuths, ranges and terrain features.

**Keywords:** *radar, directional pattern, rear lobe, “false” landmark, digital terrain model*

**Introduction.** The advent of accessible digital terrain maps, such as [1, 2] and their constant improvement [3, 4] made it possible to create radar models of reflections from local objects that can be used for terrain orientation [5, 6]. Radar orientation in the space of aerial objects has been developing successfully for a long time [7, 8]. However, specific problems appear with radar orientation of ground objects, one of which is associated with the appearance of “false” landmarks associated with reflections from the terrain received by the side and rear lobes of the radar directional pattern.

**Problem statement.** The orientation of the RLS on the ground using a radar signal is accompanied by certain problems associated with the directional pattern of the antenna (DPA). The presence of signals from the rear and side lobes in the diagram leads to the appearance of false images on the RLS indicator, which make it difficult, and in some cases make it impossible to identify the real picture of radar reflections formed by the main lobe. It is known that DPA is approximated by a function of the form  $F(x) = \frac{\sin x}{x}$ . It follows that the width of the main and rear lobes of the radiation pattern is twice as wide as the side lobes located next to them [9]. In this regard, special attention is paid to the establishment and suppression of signals from the rear lobe.

A feature of the image formation from the rear lobe is the appearance of false landmarks on the indicator, which are located in the opposite direction (180°) from the main lobe of the DPA at the same range. The similarity of the reflections received by the main maximum of the radiation pattern and its rear lobe makes it difficult to isolate phantom reflections in order to suppress them.

False images complicate the task of navigating the RLS on the ground. Therefore, the removal of reflected signals received by the rear lobe of the antenna is a common problem for all RLS.

**Literature review.** There are several methods for suppressing the posterior lobe of the DPA [10]. Conditionally, they can be divided into two independent approaches. In the first, the solution to the problems of the rear lobes is aimed at developing constructive and technical solutions for the creation of new RLS that allow changing the geometry of the DPA in order to reduce the intensity of radiation from the rear and side lobes. The second, focused on RLS, is aimed at identifying and suppressing signals received by the rear and side lobes without changing the geometry of the radar DPA. Antennas are used with variable directivity, which can change their orientation by adjusting the shape or geometry, which allows you to control the back radiation. It involves the use of digital signal processing algorithms to suppress interference and interference arising from the rear lobes.

Methods of distributed radiation pattern formation based on optimized elliptical arc geometry (EAG) are proposed to suppress the rear lobes of linear antenna arrays (LAA) [11,12].

In [13,14], it is proposed to use adaptive beamforming to suppress the rear lobes to detect and evaluate the signal of interest at the output of the sensor matrix through adaptive spatial filtering and interference suppression.

Of interest is the suppression of lattice lobes using antenna arrays with discrete dipole elements [15], an approach to the suppression of lattice lobes based on a null scanning antenna (NSA) for a sparse phased array [16], the synthesis of a conformal antenna array template using an optimization algorithm [17].

In [18,19], a new optimized structure of a square pyramidal antenna array is proposed to minimize the back lobe of flat antenna arrays. The problem of uniformity of the amplitude of

the main beam an additional structure is proposed that allows minimizing the rear lobe, while maintaining control over such characteristics of the radiation pattern as the level of the side lobes and the beam width of half power.

Despite the difference in approaches to the problem of the rear lobes and the degree of success in solving it, the known methods are aimed at reducing the amplitude of the radiation of the rear lobe when designing new ones and, as practice shows, do not meet the conditions for solving the problem of increasing the accuracy of orientation with radar locations of existing RLS.

**Research methodology.** To solve the problem of identifying false landmarks and removing them, a method is proposed that effectively identifies phantom reflections and suppresses them. The idea of the method is based on the immobility of the terrain relative to the radar station during its location. This determines the appearance of phantom reflections at the same range as real reflections at angles differing by 1,800. The amplitude of the phantom reflection should be less than the real reflection received by the main lobe of the radiation pattern by as many times as the amplitude of the rear lobe is less than the amplitude of the main lobe of the radiation pattern of the radar antenna. Such signals should be ignored and removed from the radar portrait of the terrain. However, since there is a probability of finding opposite landmarks, only those signals whose level is less than the main signal by as many times as the level of the main maximum of the directional pattern is higher than the level of the rear lobe of the directional pattern should be suppressed. Since these ratios are different for different radars and at different frequencies, at the first stage of suppression, several maximum-level signals are sought in radar reflection, regardless of azimuth. Since these signals are maximum, they are obviously received by the main lobe of the radiation pattern, and the signal-to-noise ratio in the radar reflection will also be maximum, which will increase the measurement accuracy.

At azimuths opposite to the azimuths of maximum signal reception and at the same ranges, the levels of radar reflection received by the rear lobe of the radiation pattern are measured, the ratios of the levels of these signals and their average value are calculated. When false reflections are suppressed, the values received by the main radar beam, but reduced in level by the value of the calculated ratio of signal levels in the main and rear lobes of the radiation pattern, are subtracted from the signals received by the rear lobe of the radiation pattern.

In practice, there is a spread of signal ratios in the main and rear lobes of the radiation pattern, associated both with the presence of noise and interference, and with the accuracy of signal measurements by the radar radio receiver. To make a decision on the suppression of "false" reflection, not a strict threshold is used, but a threshold interval that takes into account the presence of noise and errors in RLS measurements. The introduction of such an interval can lead to the fact that after suppressing "false" reflections, negative signal levels can be obtained. To eliminate such a situation, instead of negative levels in radar reflection, such values are replaced with levels corresponding to the average value of radio noise.

To calculate the average level of radio noise required for the operation of the algorithm for suppressing "false" reflections, at least 200 signal levels ( $A_n$ ), which are measured at distances obviously greater than those at which local objects (visible hills) may be located. Calculation of the average noise level

$$\bar{A}_n = \frac{1}{N} \sum_{i=1}^N A_{ni},$$

where  $N$  is the number of received signals;  $A_{ni}$  is the level of the  $i^{\text{th}}$  signal.

The detection threshold  $A_t$  for radar is calculated using the formula

$$A_t = k_{th} \cdot \bar{A}_n, \quad (1)$$

where  $k_{th}$  is the coefficient for calculating the Detection Threshold.

We determine the signal amplitude levels for azimuth values from 0 to 180 degrees over the entire range of the RLS range. If the signal level exceeds the Detection Threshold (1), the signal level is determined at the same range at an azimuth equal to – the azimuth of the detected signal plus 180 degrees. If this signal also exceeds the Detection Threshold, then it is checked which of the signals is greater. The larger signal is considered to be the signal received by the main lobe of the antenna  $A_m$  (main), and the smaller signal is considered to be the signal received by the rear lobe of the antenna  $A_b$  (back). Calculate the ratio  $R$  of the level of the larger signal to the level of the smaller signal

$$R = \frac{A_m}{A_b}. \quad (2)$$

The ratio (2) is the basis of the criterion by which the signals from the front and rear lobes of the DPA are identified. In this regard, to establish the uniqueness of the criterion, to exclude accidental overlaps of signals, it is necessary to use the average value of the ratio  $\bar{R}$ . To do this, a set of  $R_i$  ratios corresponding to different azimuth and range values is used, subject to the maximum  $A_{mi}$  condition. The number of ratios  $M$  is determined by the spread in the values of  $R_i$

$$\bar{R} = \frac{1}{M} \sum_{i=1}^{i=N} R_i. \quad (3)$$

For each received  $A_i$  signal, the conditions for exceeding the detection threshold  $A_t$  are checked

$$A_i(\varphi); A_i(\varphi + \pi) \geq A_t.$$

If the condition is met, then the conditions are checked

$$A_i(\varphi) \geq A_i(\varphi + \pi). \quad (4)$$

If condition (4) is met, the  $A_i(\varphi)$  signal is considered to be received by the main lobe of the DPA. The signal  $A_i(\varphi + \pi)$  is received by the rear lobe of the antenna. If condition (4) is not fulfilled, the signal  $A_i(\varphi)$  is considered to be received by the rear DPA. The signal  $A_i(\varphi + \pi)$  is received by the main lobe. We calculate the ratio of the larger signal to the smaller  $K$ . Then we check whether the calculated ratio  $K$  falls into the following range

$$R - R \cdot k_R \geq K \geq R + R \cdot k_R. \quad (5)$$

For the average value  $\bar{R}$  (3)

$$\bar{R} - \bar{R} \times k_R \geq K \geq \bar{R} + \bar{R} \times k_R, \quad (6)$$

where  $k_R$  is the coefficient determining the level of signal suppression, which is set experimentally. It follows from conditions (5) and (6) that  $k_R$  defines the range between the upper and lower bounds of these inequalities, defined as  $2R \cdot k_R$  and therefore is very important in the implementation of back lobe suppression.

If the calculated  $K$  ratio falls within the specified range, we assume that the smaller signal ( $A_{back}$ ) is a signal reflected from a Local Object, received by the rear lobe of the antenna, and reduce it to the value of the average noise amplitude ( $A_{Noise}$ ).

If the calculated ratio is less than the specified range, we assume that the smaller signal ( $A_{Back}$ ) is the signal reflected from the Local Object, received by the rear lobe of the antenna, plus an additional signal, and reduce it to the  $A_{im}$  value according to the following formula

$$A_{im}(\varphi) = (\varphi) - \frac{A_i(\varphi + \pi)}{R}. \quad (7)$$

Using  $\bar{R}$  (4), expression (7) is written as



The red color on the graph shows the levels of the reflected signal received by the front lobe, the green color shows the back lobe.

The signal levels are given in units of the ADC (analog-to-digital converter) of the receiving device. The main maximum of the front lobe is directed at azimuth  $0^\circ$ ,  $k_n = 5$ ,  $k_R = 0.2$ .

At these coefficient values, the amplitude of the signal received by the rear lobe after suppression decreases by 45 %. Fig. 3 shows images of the RLS all-round view indicator before and after the suppression of the signal received by the rear lobe.

Figs. 4, 5 and 6 show the amplitudes of the signals after the suppression of the rear lobes at various values of  $k_R$  and the corresponding images of the RLS all-round view indicators and the main maximum of the front lobe directed at azimuth  $0^\circ$  at  $k_n = 5$ . Determining the optimal values of  $k_n$  and  $k_R$  allows you to simultaneously maintain the level of useful signals while suppressing false ones. To fulfill this condition, the most important thing is to establish the effective value of the  $k_R$  coefficient, which determines the level of signal suppression, which is set experimentally.

Thus, at values  $k_n = 5$ ,  $k_R = 0.6$ , the amplitude of the signal received by the rear lobe after suppression decreases by 83 %.

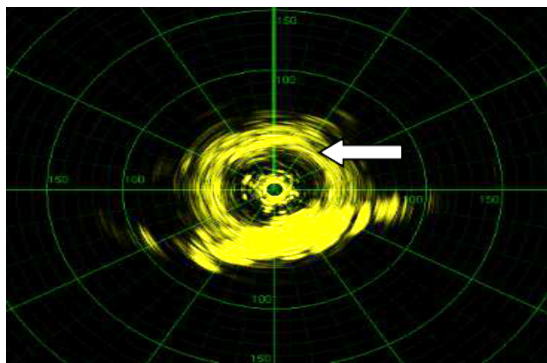
At these values, the amplitude of the signal received by the rear lobe after suppression decreases by 94 %.

At these values, the amplitude of the signal received by the rear lobe after suppression decreases to almost zero.

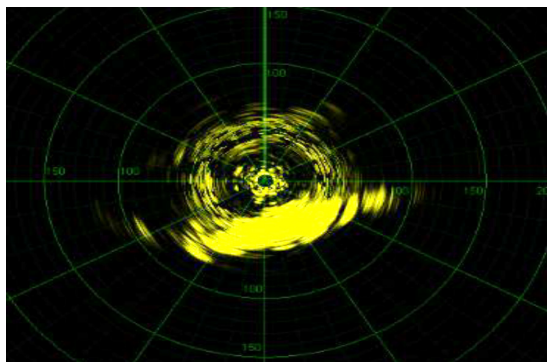
At the same RLS radiation frequency, the suppression of false signals generated by the rear lobe at an azimuth of 150 degrees and a frequency of 145 MHz and a noise factor of 5 at different values of  $k_R$  were investigated, Fig. 7.

The green color on the graph shows the levels of the reflected signal received by the front lobe, the red color shows the side and rear lobes.

Thus, the signal amplitude at an azimuth of 150 degrees and a frequency of 145 MHz and a noise factor of  $k_n = 5$  after suppression decreases at  $k_R = 0.2$  by 47 %, with  $k_R = 0.6$  by 84 %. A

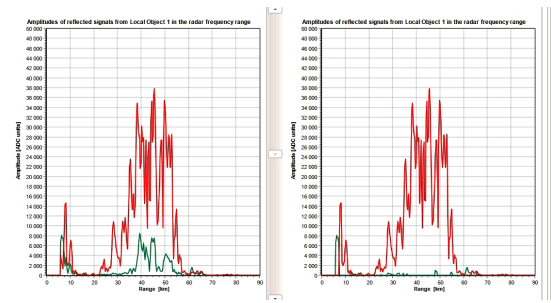


a

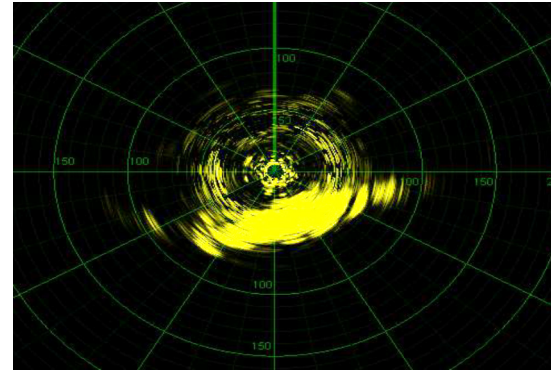


b

Fig. 3. General radar picture: a – without suppression of the posterior lobe; b – after suppression. The arrow points to false reflections

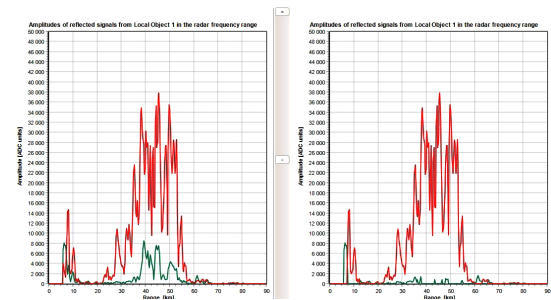


a

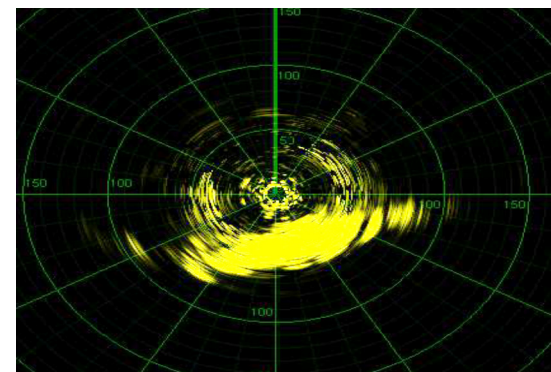


b

Fig. 4. Signal amplitudes (a) and radar image (b), with back lobe suppression at  $k_R = 0.6$



a



b

Fig. 5. Signal amplitudes (a) and radar image (b), with back lobe suppression at  $k_R = 1$

further increase in  $k_R$  does not change the signal level. Comparative analysis of the suppression of the signal of the rear lobe at azimuths of 0 degrees and 150 degrees shows the independence of the results from the direction of the main lobe.

### Conclusions.

1. The proposed method makes it possible to suppress “false” reflections from the rear lobe without having a priori information about the real directional pattern.

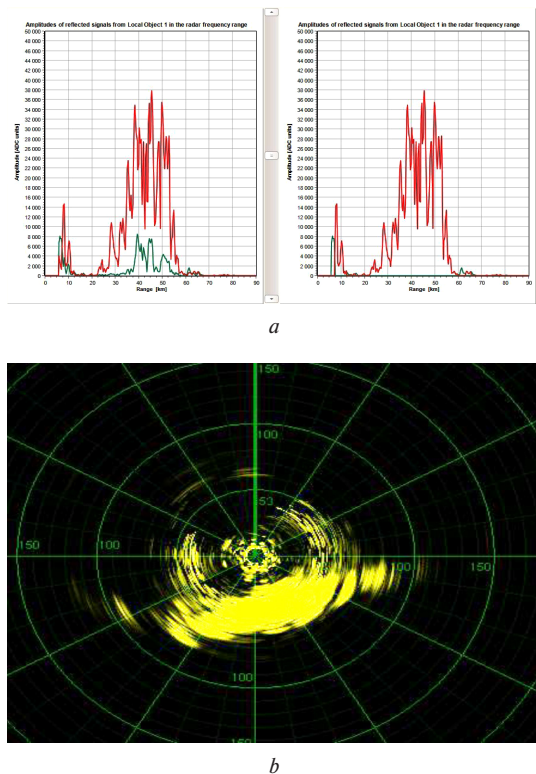


Fig. 6. Signal amplitudes (a) and radar image (b), with back lobe suppression at  $k_R = 1.2$

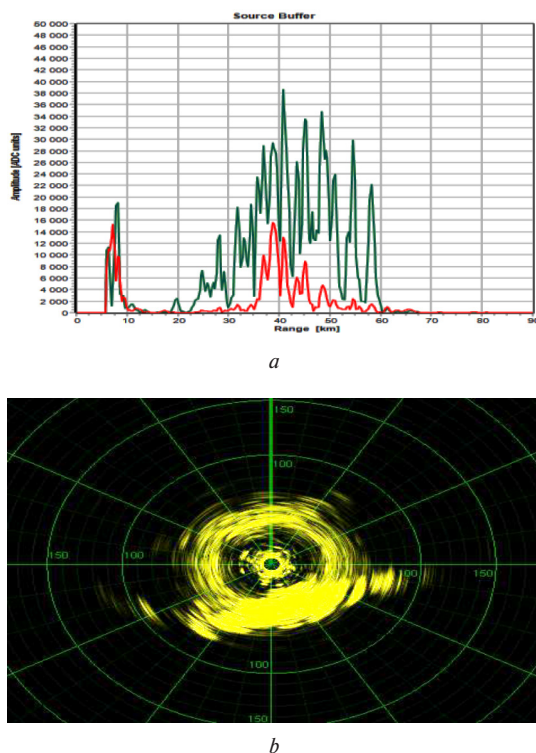


Fig. 7. Signal amplitudes (a) and a snapshot of the ICO (b) without suppression of the side and rear lobes

2. A new approach to suppression of the rear lobe of the DPA based on a criterion determined by the ratio of the amplitude of the signal received by the front lobe to the amplitude of the signal received by the rear lobe ( $R_{\text{calculated}} = A_{\text{main}}/A_{\text{back}}$ ) and the suppression level regulator has shown its effectiveness and ability to suppress the rear lobe to zero.

3. The computational potential of the developed computer program for the implementation of the solution of the task has shown its promise and determines the possibility of its use on any type of radar at various frequencies and ranges.

4. After suppressing reflections from the back lobe, “false” reflections remain, formed by the side lobes, the removal of which requires the development of additional methods.

**Acknowledgments.** This article is based on the results of research on the topic “Development of methods of ground-based radar navigation” IRN No. AP148036/0222.

#### References.

1. Global digital elevation model ASTER V003 (n.d.). Retrieved from [https://search.earthdata.nasa.gov/search/granules?p=C1711961296-LPCLOUD&pg\[0\]\[v\]=f&pg\[0\]\[gsk\]=-start\\_date&fi=ASTER&tl=1705558986.6823!!!](https://search.earthdata.nasa.gov/search/granules?p=C1711961296-LPCLOUD&pg[0][v]=f&pg[0][gsk]=-start_date&fi=ASTER&tl=1705558986.6823!!!).
2. Earthdata Search/ Earthdata Search (n.d.). Retrieved from <https://search.earthdata.nasa.gov/search/?fi=ASTER&tl=1705558986.6823!!!>.
3. Saritha, G., Saravanan, T., Anbumani, K., & Surendiran, J. (2021). Digital elevation model and terrain mapping using LiDAR. *International Conference on Materials, Manufacturing and Mechanical Engineering for Sustainable Developments-2020 (ICMSD 2020)*, 46(9), 3979-3983. <https://doi.org/10.1016/j.matpr.2021.02.525>.
4. Imansakipova, B. B., Orynbasarova, E. O., Sdvizhkova, O. O., Aitkazinova, S. K., & Shoganbekova, D. A. (2022). A new approach to improving the accuracy of measuring deformations of the earth's surface using space radar interferometry methods. *Proceedings of the international scientific and practical conference*, 2, 88-94. Retrieved from <https://official.satbayev.university.ru/materialy-satpaevskikh-chteniy>.
5. Mahmoud El Nokrashy O. Ali, Lamyaa Gamal EL-Deen Taha, Mostafa H. A. Mohamed & Asmaa A. Mandouh (2021). Generation of digital terrain model from multispectral LiDAR using different ground filtering techniques. *The Egyptian Journal of Remote Sensing and Space Sciences*, 24(2), 181-189 <https://doi.org/10.1016/j.ejrs.2020.12.004>.
6. Imansakipova, B. B., Vasiliev, I. V., Aitkazinova, Sh. K., & Kaliparov, M. M. (2023). Using a digital terrain model to orient a radar antenna system. *PROCEEDINGS of the International Scientific and Practical Conference "INTERNATIONAL SATBAYEV CONFERENCE"*, 1. Almaty 2023. 65-72. <https://doi.org/10.51301/ejsu.2022.i6.01>.
7. Scannapieco, A. F., Graziano, M. D., Fasano, G., & Renga, A. (2019). Improving radar-based mini-UAS navigation in complex environments with outlier rejection. *AIAA Scitech 2019 Forum*. Retrieved from [https://www.researchgate.net/publication/330196408\\_Improving\\_radar-based\\_mini-UAS\\_navigation\\_in\\_complex\\_environments\\_with\\_outlier\\_rejection](https://www.researchgate.net/publication/330196408_Improving_radar-based_mini-UAS_navigation_in_complex_environments_with_outlier_rejection).
8. Scannapieco, A. F., Renga, A., Fasano, G., & Moccia, A. (2017). Ultralight radar for small and micro-UAV navigation. *International Archives of the Photogrammetry, Remote Sensing and Spatial Information Sciences – ISPRS Archives*, 42(2W6), 333-338. Retrieved from [https://www.researchgate.net/publication/319413337\\_ULTRA-LIGHT\\_RADAR\\_FOR\\_SMALL\\_AND\\_MICRO-UAV\\_NAVIGATION](https://www.researchgate.net/publication/319413337_ULTRA-LIGHT_RADAR_FOR_SMALL_AND_MICRO-UAV_NAVIGATION).
9. Kavita Devi & Rajneesh Talwar (2017). A Neural Adaptive Circular Array for Enhancing SNR and Reducing Interference. *International Journal of Computer Sciences and Engineering*, 5(10), 122-127. <https://doi.org/10.26438/ijcse/v5i10.122127>.
10. Balanis, C. A. (2016). *Antenna Theory: Analysis and Design* (4<sup>th</sup> ed.). ISBN: 978-1-118-64206-1.
11. Dawood, H. S., El-Khobby, H. A., Abd Elnaby, M. M., & Hussein, A. H. (2022). New distributed beamforming techniques based on optimized elliptical arc geometry for back lobe cancellation of linear antenna arrays. *Alexandria Engineering Journal*, 61(6), 4623-4645. <https://doi.org/10.1016/j.aej.2021.10.024>.
12. Silveira, E. S., Nascimento, D. C., & Tinoco-S, A. F. (2017). Design of Microstrip Antenna Array with Suppressed Back Lobe. *Journal of Microwaves, Optoelectronics and Electromagnetic Applications*, 16(2). <https://doi.org/10.1590/2179-10742017v16i2822>.
13. Gu, Yu., Goodman, N. A., Hong, S., & Li, Y. (2014). Robust adaptive beamforming based on interference covariance matrix sparse reconstruction. *Signal Processing*, 96(Part B), 375-381. <https://doi.org/10.1016/j.sigpro.2013.10.009>.
14. Chakravorty, P., & Mandal, D. (2016). Grating Lobe Suppression With Discrete Dipole Element Antenna Arrays. *IEEE Antennas and Wireless Propagation Letters*, 15, 1234-1237. <https://doi.org/10.1109/LAWP.2015.2502902>.

15. Ding, Z., Chen, J., Liu, H., He, C., & Jin, R. (2022) Grating Lobe Suppression of Sparse Phased Array by Null Scanning Antenna. *IEEE Transactions on Antennas and Propagation*, 70(1), 317-329. <https://doi.org/10.1109/TAP.2021.3090573>.
16. Prabhakar, D., & Satyanarayana, M. (2019). Side lobe pattern synthesis using hybrid SSWOA algorithm for conformal antenna array. *Engineering Science and Technology, an International Journal*, 22(6), 1169-1174. <https://doi.org/10.1016/j.jestch.2019.06.009>.
17. Dawood, H. S., El-Khobby, H. A., Abd Elnaby, M. M., & Hussein, A. H. (2022). A new optimized quadrant pyramid antenna array structure for back lobe minimization of uniform planar antenna arrays. *Alexandria Engineering Journal*, 61(8), 5903-5917. <https://doi.org/10.1016/j.aej.2021.11.018>.
18. Ullah, N., Liu, Yu., Ur Rahman, S., Khan, S., & Wang, F. (2024). Design of a compact filter integrated wideband and circularly polarized antenna array for K-band application. *Measurement*, 225. <https://doi.org/10.1016/j.measurement.2023.113978>.
19. Jarboua, I., Ammar, N., Aguil, T., & Baudrand, H. (2019). Radiation pattern and scattering parameter for multilayer cylindrical loop antenna using the iterative method WCIP. *International Journal of Electronics and Communications*, 101, 192-199. <https://doi.org/10.1016/j.aeue.2019.01.024>.

## Ідентифікація та пригнічення сигналів задньої пелюстки діаграми спрямованості антени радара

Б. Б. Імансакінова<sup>1</sup>, І. В. Васильєв<sup>2</sup>,  
Ш. К. Айтказінова<sup>\*1</sup>, М. М. Каліпанов<sup>3</sup>, К. Ж. Ісабаєв<sup>3</sup>

1 – НАТ «Казахський національний дослідницький технічний університет імені К.І. Сатпаєва», м. Алмати, Республіка Казахстан

2 – Спеціальне конструкторсько-технологічне бюро «Граніт», м. Алмати, Республіка Казахстан

3 – Інституту машинознавства та автоматики Національної академії наук Киргизької Республіки, м. Бішкек, Киргизька Республіка

\* Автор-кореспондент e-mail: [sh.aitkazanova@satbayev.university](mailto:sh.aitkazanova@satbayev.university)

**Мета.** Розробка нового підходу до підвищення точності орієнтування по радіолокаційним відбиттям від місцевих об'єктів і цифрової моделі місцевості.

**Методика.** Дослідження засновані на теорії випромінювання, відбиття та прийняття радіолокаційних сигналів. Статистичний аналіз великого обсягу реєстрованих сигналів дозволяє встановити причинно-наслідкові зв'язки появи «помилкових» відображень, що формуються задньою пелюсткою діаграми спрямованості, і розробити обчислювальний алгоритм їх пригнічення.

**Результати.** Розроблені метод і програмне забезпечення, що дозволяють виявляти та пригнічувати «помилкові» відображення, які формуються задньою пелюсткою діаграми спрямованості антени, не спотворюючи відображення від головної пелюстки. Для цього розроблено критерій, який визначається відношенням амплітуди сигналу, прийнятого передньою пелюсткою, до амплітуди сигналу, що реєструється задньою пелюсткою. Критерій дозволяє виключити «помилкові» сигнали, не маючи апріорної інформації про реальну діаграму спрямованості, за допомогою регулятора, що обрізає фантомні відображення до середнього рівня шумових перешкод.

**Наукова новізна.** Уперше здійснене пригнічення фантомних відображень при відсутності апріорної інформації про діаграму спрямованості антени радіолокаційної станції, виключення втрати інформативності реального відображення, сформованого головною пелюсткою.

**Практична значимість.** Запропоновано метод перешкодозахищеності радіолокаційних станцій у зв'язку з «помилковими» відображеннями. Потенціал методу й можливості розробленої комп'ютерної програми зумовлюють їх затребуваність для використання всіма радіолокаційними станціями при різних частотах, азимутах, дальностях і особливостях рельєфу місцевості.

**Ключові слова:** радіолокація, діаграма спрямованості, задня пелюстка, «помилковий» орієнтир, цифрова модель місцевості

*The manuscript was submitted 06.02.24.*